Materials Horizons

COMMUNICATION

View Article Online
View Journal | View Issue

Cite this: *Mater. Horiz.*, 2019, 6, 1463

Received 13th February 2019,
Accepted 8th April 2019

DOI: 10.1039/c9mh00230h

rsc.li/materials-horizons

Rational design of one-dimensional hybrid organic–inorganic perovskites with room-temperature ferroelectricity and strong piezoelectricity†

Daibei Yang,[ab] Lingheng Luo,[ab] Yi Gao,[c] Shuang Chen *[ad] and Xiao Cheng Zeng *[ef]

Rational design of ferroelectric/piezoelectric materials is still a big challenge due to our incomplete understanding of the underlying phase-transition mechanisms. Herein, by using first-principles calculations, three prototypes of one-dimensional (1D) hybrid organic–inorganic perovskites (HOIPs) as benchmarks are investigated, from which an approach to measure their ferroelectricity/piezoelectric-related key parameters is developed. Specifically, the ferroelectric transition temperature can be assessed by the computed energies and polarizations, and the piezoelectricity can be evaluated by the change of lattice parameters β during the phase transition. Based on this computational approach, we have examined a series of organic cations to design new 1D HOIPs *via* conscious chemical modification. Among them, seven potential candidates with excellent ferroelectricity or piezoelectricity are identified, especially for two of them, trimethyl-(2,2,2-trifluoroethyl)ammonium trichloromanganese(II) (TMTFE-$MnCl_3$) and diethylmethyl(2-fluoroethyl)ammonium trichloromanganese(II) (DEMFE-$MnCl_3$). We predict that the TMTFE-$MnCl_3$ and DEMFE-$MnCl_3$ crystals outperform all previously reported 1D ferroelectric HOIPs in terms of high spontaneous polarization, high phase transition temperature, and strong piezoelectricity. The newly proposed design strategy for 1D HOIPs with room-temperature ferroelectricity or strong piezoelectricity can be validated for broader applications if both outstanding ferroelectric/piezoelectric perovskites can be synthesized and confirmed in the laboratory.

New concepts

The marriage of inorganic and organic components in hybrid organic–inorganic perovskites (HOIPs) can bring new functional materials with technological opportunities. One remarkable example is the three-dimensional (3D) HOIPs as photovoltaic absorbers. Here, 1D HOIPs with specific linear anionic chains are predicted to possess excellent ferroelectricity and even piezoelectricity. The ferroelectric, piezoelectric, and dielectric responses of 1D HOIPs hinge on variation of the microscopic structure with temperature. Based on the first-principles computation of three model systems, the phase transition mechanism is predicted to be through molecular motions of organic cations along with translation and tilt of inorganic $MnCl_3$ anionic chains. The computation allows us to obtain ferroelectricity and piezoelectricity related physical parameters and to guide rational design of organic cations for new 1D HOIPs. Seven 1D ferroelectric/piezoelectric HOIPs are identified for future experimental confirmation. In particular, two 1D HOIPs are found to have exceptional ferroelectricity and piezoelectricity, outperforming all previously reported 1D perovskites. Our design strategy can have important implications for the development of novel perovskites with a similar phase-transition mechanism.

Introduction

Ferroelectrics represent a unique class of materials that can exhibit spontaneous polarization (P_s) below the Curie temperature (T_c), while P_s can be switched by an applied external electric field. Ferroelectrics are intrinsically piezoelectric due to their lack of an inversion center. Piezoelectric materials can realize the interconversion between electric voltage and mechanical stress. Thus far, it has been found that many inorganic ferroelectrics (*e.g.*, lead zirconate titanate (PZT) and barium titanate (BTO)) possess excellent piezoelectricity, as well as coupled electronic and optoelectronic properties, thereby greatly expanding their capabilities for device applications.[1] However, pure inorganic ferroelectrics

[a] *Kuang Yaming Honors School, Nanjing University, Nanjing, Jiangsu, 210023, China. E-mail: chenshuang@nju.edu.cn*
[b] *School of Chemistry and Chemical Engineering, Nanjing University, Nanjing, Jiangsu 210023, China*
[c] *Division of Interfacial Water and Key Laboratory of Interfacial Physics and Technology, Shanghai Institute of Applied Physics, Chinese Academy of Sciences, Shanghai 201800, China*
[d] *Institute for Brain Sciences, Nanjing University, Nanjing 210023, China*
[e] *Department of Chemistry, University of Nebraska–Lincoln, Lincoln, Nebraska 68588, USA. E-mail: xzeng1@unl.edu*
[f] *Department of Mechanical and Materials Engineering, University of Nebraska–Lincoln, Lincoln, Nebraska 68588, USA*

† Electronic supplementary information (ESI) available: Computational details, phase-transition-related structural parameter changes and summarized theoretical and experimental 1D HOIPs. See DOI: 10.1039/c9mh00230h

are hard to process, and many of them are not bio-friendly due to the inclusion of toxic rare-earth metal cations. Since 2005,[2] pure organic ferroelectrics have been brought to bear, featuring "soft" mechanical characteristics. By and large, organic ferroelectrics are light, flexible, easily processible, nearly nontoxic, biocompatible, and inexpensive. Until now, except for poly(vinylidene fluoride) (PVDF), most organic ferroelectrics are still far from realistic device applications due to their low spontaneous polarization, low Curie temperature, and absent multipolar axes. In addition, most organic ferroelectrics are very weak in piezoelectric response.[3] Recently, hybrid organic–inorganic perovskites (HOIPs) have achieved major advances in solar-cell research,[4–6] particularly, methylammonium lead iodide ($MAPbI_3$) and formamidinium lead iodide ($FAPbI_3$).[7,8] The combined inorganic and organic components in HOIPs are expected to exhibit integrated multifunctional properties, such as optoelectronic properties, ferroelectricity, and piezoelectricity, as well as easy chemical variability and structural tunability, which would offer greater opportunities for realistic device applications than those of either pure inorganic or pure organic ferroelectrics.

Many bulk HOIPs can be described by a general chemical formula of ABX_3, where A represents organic cations with different sizes and different valence states, and B represents metal cations which are typically six-coordinated with the X anions to form a BX_6 octahedron. If these BX_6 octahedra are corner-shared, A-site cations are located in cavities between the octahedra to form three-dimensional (3D) HOIPs. With facile chemical modification, the BX_6 octahedra can also be face-shared to form infinite one-dimensional (1D) linear anionic chains separated by specific A cations. As such, a new subclass of ferroelectric HOIPs, namely, 1D perovskites, can be synthesized[3,9–16] to further tune the multifunctional antiferroelectricity,[11] piezoelectricity,[3,12,13] multiferroicity,[14] photoluminescence,[10,14,15] and nonlinear optical switches.[16] Among these 1D ferroelectric perovskites with an ABX_3 formula,[3,9–16] the polar A cations are typically monovalent organic ammonium cations, categorized into two types, (1) quasi-planar 5-membered-ring, *e.g.*, pyrrolidinium and 3-pyrrolinium; and (2) quasi-spherical, *e.g.*, trimethylchloromethylammonium (TMCM) and trimethylbromomethylammonium (TMBM), as exemplified in Fig. 1. The B cations are divalent metal cations, and only Mn^{2+} and Cr^{2+} ions are identified here to form these 1D ferroelectric perovskites. Lastly, the X anions are the halogen elements, Cl^- or Br^-.

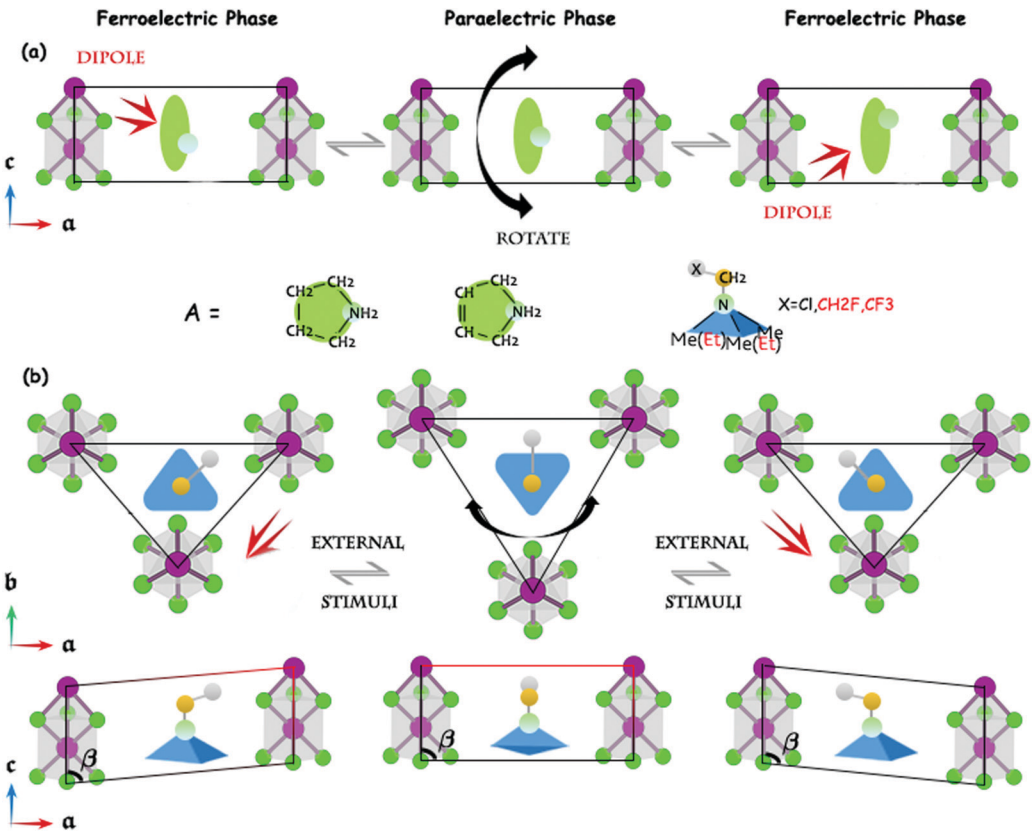

Fig. 1 Phase-transition mechanisms of 1D ferroelectric $AMnCl_3$ perovskites, changing alternatively between ferroelectric phase and paraelectric phase. The 1D chains with purple and green atoms denote the $MnCl_3$ anions. Here, A stands for organic cations, including (a) quasi-planar pyrrolidinium and 3-pyrrolinium and (b) quasi-spherical trimethylchloromethylammonium (TMCM), trimethyl(2,2,2-trifluoroethyl)ammonium (TMTFE), and diethylmethyl(2-fluoroethyl)ammonium (DEMFE). For these organic cations, their chemical formulas are highlighted in the insets, where the substituent groups in red color are newly proposed by design. The organic cations are located within the triangular plane formed by three 1D $MnCl_3$ chains (along *c* axis), as highlighted in the top view of the TMCM-$MnCl_3$ crystal (see upper panels of (b)). The red arrows denote the dipole moments of the organic cations. The black arrows mark the thermal motions of organic cations in the paraelectric phase. The crystal axes (*a*, *b*, or *c*) are also highlighted in the insets. The lower panels in (b) are side views of the TMCM-$MnCl_3$ crystal.

The experimentally-synthesized 1D HOIPs exhibit excellent ferroelectricity with high transition temperature T_c and low coercive field E_c,[3,9–16] and even exceptional piezoelectricity with a very large d_{33} coefficient that is comparable to that (190 pC N^{-1} along the [111] direction) of single-crystal BTO.[3] These materials mostly have a spontaneous polarization of a few μC cm^{-2},[3,9–16] which can be less than those of pure inorganic ferroelectrics, but is still quite good. It is known that ferroelectrics can undergo temperature-induced structural phase transition from a centrosymmetric high-temperature phase (HTP) to a non-centrosymmetric low-temperature phase (LTP).[15] For ferroelectric perovskites shown in Fig. 1, the HTP corresponds to a paraelectric phase, and the LTP corresponds to a ferroelectric phase. Thus, the Curie temperature, T_c, above which the ferroelectrics lose their spontaneous polarizations, is the phase transition temperature. This phase transition is also associated with the emergence of a large piezoelectric coefficient below T_c.[3] The X-ray diffraction (XRD) analyses indicated that the phase transition of 1D ferroelectric perovskites is due to the freezing of dynamic organic cations and subsequent alignment of their dipole moments below T_c.[9,12,13,16] During the phase transition, the intrachain structure of BX_6 chains is almost unchanged.[16,17] It is believed that the ferroelectric-to-paraelectric phase transition is largely attributed to thermal activation, and thus the height of the energy barrier separating the two phases in an energy diagram is related to T_c.[11,18] The T_cs of most 1D HOIPs are higher than 240 K.[3,9–16]

Remarkably, the transition temperatures of 1D TMCM-$MnCl_3$ and TMBM-$MnBr_3$ crystals can reach 406 K[3] and 415 K,[12] respectively, much higher than the room temperature. High T_c is critical to practical applications of ferroelectrics. From the polarization–electric field (*P*–*E*) hysteresis loop, we learn that the net polarization becomes zero at the coercive field E_c, implying that the volume fractions of the domains with opposite directions are the same. Most 1D ferroelectric HOIPs have quite small E_cs, typically a few kV cm^{-1},[3,9–16] which are lower than those of most organic ferroelectrics and metal–organic ferroelectrics, and are three orders of magnitude lower than that of polymer ferroelectrics.[9] When the organic cations are changed from quasi-planar pyrrolidinium or 3-pyrrolinium to quasi-spherical TMCM or TMBM, 1D ferroelectric perovskites acquire excellent piezoelectricity.[3,12,13] TMCM-$MnCl_3$,[3] TMBM-$MnBr_3$,[12] and TMCM-$CdBr_3$[13] crystals all possess a large d_{33} (larger than 112 pC N^{-1}), and their transition temperatures are higher than 346 K.

The ferroelectric, piezoelectric, and dielectric responses of 1D HOIPs are all sensitive to variation of the microscopic structure with temperature. For rational design of 1D HOIPs, we chose three model systems as benchmarks (Fig. 1), namely, (pyrrolidinium)$MnCl_3$,[10] (3-pyrrolinium)$MnCl_3$,[15] and TMCM-$MnCl_3$,[3] to investigate their property-correlated phase transition mechanisms. All these three model systems have been experimentally well characterized and all have the same inorganic $MnCl_3$ anionic chains. The change of organic cations from quasi-planar pyrrolidinium and 3-pyrrolinium to quasi-spherical TMCM can additionally give rise to ultra-large piezoelectricity.[3,10,15] By using the climbing-image nudged elastic band (CI-NEB) calculations, the phase-transition mechanisms of these three model systems could be illustrated at the molecular level. For the first type of 1D perovskites as shown in Fig. 1a, both (pyrrolidinium)$MnCl_3$[10] and (3-pyrrolinium)$MnCl_3$[15] entail similar phase-transition mechanisms by which organic cations sway around their molecular rings but still retain their weak hydrogen bonding with Cl atoms. However, this swing-like motion would induce weak N–H···Cl hydrogen bonding with different Cl atoms in the $MnCl_3$ chains in either the ferroelectric phase or the paraelectric phase. Above T_c, thermal energy activates the motion of organic cations to revoke their dipole moments. Below T_c, the organic cations can reorient to induce the dipole alignment, giving rise to spontaneous polarization. The second type of 1D ferroelectric perovskite, TMCM-$MnCl_3$[3] as shown in Fig. 1b, is quite different from the first type. Within this crystal, Cl atoms of the quasi-spherical TMCM cations form halogen···halogen bonds with the Cl atoms of inorganic anions. The phase-transition mechanism is still attributed to molecular motion of the organic cations, *i.e.*, rotating along the N–C methylene bond (the pseudo threefold axis of the cation) and tumbling along the *c* axis of the crystal. In both cases, translation of the $MnCl_3$ chains, especially within the *ab*-plane, could be triggered by the motion, such as swing, rotation, or tumble, of organic cations. Here, the increase of polarization below T_c is resulted from the gradual freezing of molecular motions to induce symmetry breaking. These proposed two phase-transition mechanisms supply sufficient information to analyze ferroelectricity and piezoelectricity of three model systems, and to further build the structure–property relationship of the 1D ferroelectric HOIPs. The insights obtained from this analysis are gathered to form useful principles which allow us to finally perform molecular design of organic cations, from which two new 1D ferroelectric HOIPs, namely, trimethyl(2,2,2-trifluoroethyl)-ammonium trichloromanganese(II) (TMTFE-$MnCl_3$) and diethylmethyl(2-fluoroethyl)ammonium trichloromanganese(II) (DEMFE-$MnCl_3$), are predicted with notably improved ferroelectricity and piezoelectricity.

Results and discussion

Phase transition mechanism

According to the structural characteristics of polar organic cations, three model systems of 1D ferroelectric HOIPs can be classified into two types to illustrate their phase-transition mechanisms, as shown in Fig. 1. For the first type, both organic cations, pyrrolidinium and 3-pyrrolinium, have quasi-planar molecular structures. For (pyrrolidinium)$MnCl_3$ and (3-pyrrolinium)-$MnCl_3$ crystals, their ferroelectric properties have been accurately measured in the previous experiments: (pyrrolidinium)$MnCl_3$ has P_s = 5.5 μC cm^{-2} and $T_c \approx$ 291 K,[10] while (3-pyrrolinium)$MnCl_3$ has P_s = 6.2 μC cm^{-2} and T_c = 376 K.[15] Like most organic ferroelectrics, neither system exhibits strong piezoelectricity.[10,15] On the basis of the CI-NEB calculations, the phase-transition mechanisms of (pyrrolidinium)$MnCl_3$ and (3-pyrrolinium)$MnCl_3$ crystals are illustrated in Fig. 2a, where both are due to the

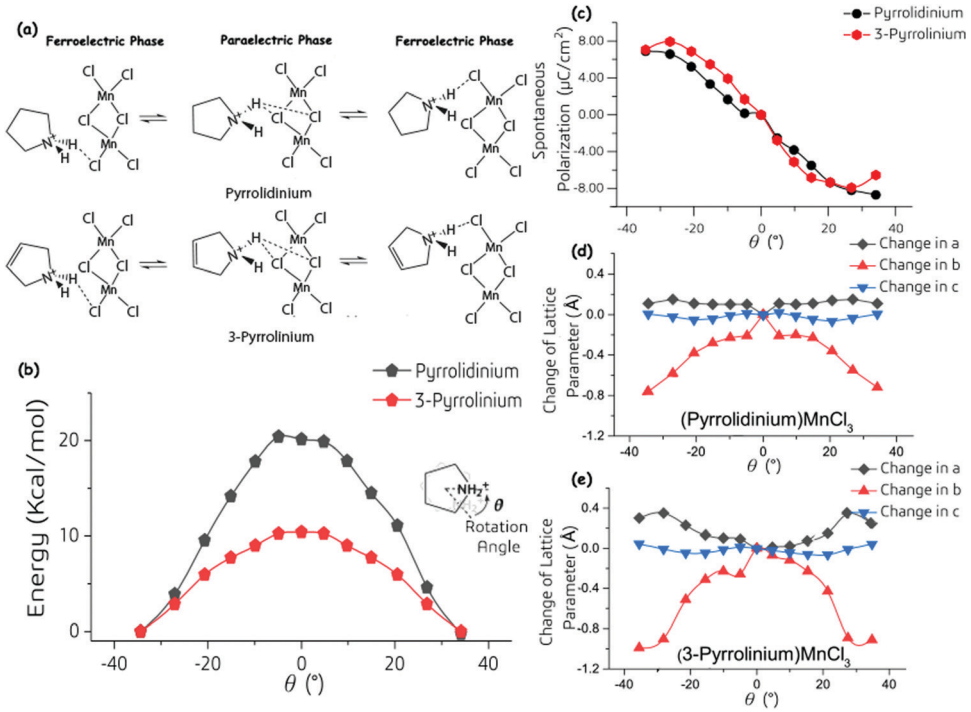

Fig. 2 (a) Molecular diagram to illustrate the phase-transition mechanism associated with the (pyrrolidinium)$MnCl_3$ and (3-pyrrolinium)$MnCl_3$ crystals; (b) variation of the energy with rotation angle θ, during the phase transition; (c) variation of spontaneous polarization with θ; (d) the lattice parameter change of the (pyrrolidinium)$MnCl_3$ crystal *versus* θ; and (e) lattice parameter change of the (3-pyrrolinium)$MnCl_3$ crystal *versus* θ. During the phase transition, the changed hydrogen bonds between organic cations and inorganic $MnCl_3$ chains are highlighted in the inset of (a). The rotation angle is defined as the azimuthal angle between the molecular axis (defined as a connecting line from center of mass toward N atom of the organic cation) of the organic cation in the ferroelectric phase and the molecular axis in the paraelectric phase, as highlighted in the inset of (b).

order–disorder transition of the organic cations, consistent with the experimental XRD analyses.[10,15]

Above T_c, the thermal activation allows strong structural fluctuation of pyrrolidinium or 3-pyrrolinium cations, swinging about their ring planes within a range of -35° to 35° rotation angle θ (Fig. 2b). The θ is defined as the azimuthal angle between the molecular axis (defined as a connecting line from center of mass toward N atom of the organic cation) of the organic cation in the ferroelectric phase and the molecular axis in the paraelectric phase. Further learned from details of N–H···Cl hydrogen bonds during the phase transition in (pyrrolidinium)$MnCl_3$ or (3-pyrrolinium)$MnCl_3$ (Fig. S3, ESI†), we found that organic cations sway around their molecular rings but still retain their weak hydrogen bonding with different Cl atoms of the $MnCl_3$ chains in either the ferroelectric phase or in the paraelectric phase. Details of the hydrogen bonds can be illustrated in Section II in the ESI.†

During the phase transition, the order–disorder motion of organic cations synergistically induces the translation between 1D inorganic $MnCl_3$ chains within the *ab*-plane without their distortion. As shown in Table S1 (ESI†), the phase transition pathway of (3-pyrrolinium)$MnCl_3$ from the ferroelectric phase to the paraelectric phase is taken as an example to highlight possible distortion-related structural parameter changes of inorganic $MnCl_3$ anions. During this phase transition, different Cl–Mn–Cl bond angles of 1D anionic chains change within the range of 1.2°, while nearly all Cl–Mn bond lengths are unchanged. Thus, we confirm that the phase transition of 1D HOIPs is independent of inorganic lattice distortion. Moreover, the translation of inorganic chains within the *ab*-plane does occur. As indicated by Fig. 2d and e, the (pyrrolidinium)$MnCl_3$ crystal has nearly constant lattice parameters, *a* and *c*, whereas its lattice parameter *b* can exhibit a large change of 0.8 Å from the ferroelectric phase to the paraelectric phase. For the (3-pyrrolinium)$MnCl_3$ crystal, its lattice parameter *c* is unchanged, while *a* becomes 0.4 Å shorter, and *b* increases 1 Å during the transition from ferroelectric to paraelectric phase. During the phase transition, the (3-pyrrolinium)$MnCl_3$ crystal is more flexible with larger change in the lattice parameters than (pyrrolidinium)$MnCl_3$, although 3-pyrrolinium cations are more rigid due to the double C–C bond than pyrrolidinium cations. The larger change in the lattice parameters of 1D HOIPs would indicate soft mechanical characteristics for potential piezoelectricity. We believe that the steric hindrance of organic cations within 1D perovskites would strongly affect their piezoelectricity.

For the transition from the ferroelectric phase (left), to the paraelectric phase, and then to the ferroelectric phase (right), the associated energy barrier is about 20.2 kcal mol^{-1} for (pyrrolidinium)$MnCl_3$ and 10.4 kcal mol^{-1} for (3-pyrrolinium)-$MnCl_3$, respectively. Here, we find that the (pyrrolidinium)$MnCl_3$ with a reported lower Curie temperature[10] actually exhibits a

higher energy barrier for phase transition (see Fig. 2b). Contrary to the suggestion that the height of the energy barrier between the ordered and disordered states is directly correlated with the transition temperature,[11,18] our computational results seem more consistent with a conclusion based on the Landau–Devonshire model,[19] that is, the height of the energy barrier separating the two phases has no obvious correlation with T_c.

According to the phase-transition pathways of (pyrrolidinium)$MnCl_3$ and (3-pyrrolinium)$MnCl_3$ crystals, the estimated variation of the spontaneous polarization with θ is shown in Fig. 2c. For the (pyrrolidinium)$MnCl_3$ crystal, the computed spontaneous polarization is in the range of -8.7 to 6.7 μC cm^{-2}, consistent with the experimental value of 5.5 μC cm^{-2}.[10] For the (3-pyrrolinium)$MnCl_3$ crystal, the spontaneous polarization ranges from -7.9 to 7.9 μC cm^{-2}, again consistent with the experimental value of 6.2 μC cm^{-2}.[15] In the paraelectric phase, both crystals have zero polarization. Changing from the ferroelectric phase (left) to the paraelectric phase, the spontaneous polarization gradually decreases as θ increases. As we know, the linear $MnCl_3$ chains in the 1D ferroelectric perovskites contribute to the polarization switching through translation within the *ab*-plane, stemming from swing-like motion of organic cations. In addition, our theoretical simulations show no distortion within the 1D $MnCl_3$ chains during the phase transition. Therefore, the dipole alignment of organic cations (pyrrolidinium or 3-pyrrolinium molecules) and the change of separation between the centers of the organic cation and inorganic anion predominantly determine the value of P_s. The dipole alignment during the phase transition is dependent on inherent molecular dipole moments (3.2 D for pyrrolidinium *versus* 3.4 D for 3-pyrrolinium, estimated from the quantum chemistry calculations) and the swing range of rotation angle. Even though the 3-pyrrolinium has a slightly higher dipole moment than that of pyrrolidinium, both quasi-planar organic cations have a similar swing range of rotation angle in Fig. 2b. The swing range of rotation angle is dependent on the steric hindrance of the organic cations. Noticeably, the swing range of rotation angle largely determines the change of separation between the centers of the organic cation and inorganic anion during phase transition, and finally affects the polarization. To achieve large polarization through rational design, it would be more effective to alter the steric hindrance of the organic cations, rather than to enlarge the dipole moment. The inorganic anions exhibit symmetry of octahedral geometry, and thus it is not workable to change the transition metal and halogen of inorganic anions to realize large polarization of 1D ferroelectric perovskites.

By replacing polar organic cations with quasi-spherical TMCM or TMBM molecules, the second type of 1D ferroelectric HOIPs, *e.g.*, TMCM-$MnCl_3$ crystals, is generated to realize piezoelectricity.[3,12,13] The TMCM molecule can be viewed as a H atom of one methyl of the spherical tetramethylammonium being replaced by a Cl atom. Thus, TMCM is made up of a $-CH_2Cl$ terminal group and a triangle-pyramid-shape $-N^+(Me)_3$ group, which has quasi three-fold symmetry around the N–C methylene bond. The detailed phase-transition mechanism of the TMCM-$MnCl_3$ crystal is illustrated in Fig. 3a. Similar to the first type of 1D ferroelectric perovskites with the quasi-planar organic cations, the TMCM-$MnCl_3$ crystal also undergoes a phase transition, originated from the coupling of order–disorder dynamics of polar organic cations and long translation of inorganic chains.[3] Due to the more complex molecular structure of TMCM, molecular motions are more complicated during the phase transition. Thus, the TMCM-$MnCl_3$ crystal can exhibit two possible phase-transition pathways (Fig. 3a). One is to keep the dipole orientation of each TMCM molecule along the *c* axis unchanged, while it follows a "rotate-sway-rotate" pathway (the upper row in Fig. 3a). Here, one TMCM cation is located within the triangular plane formed by three $MnCl_3$ anionic chains. Along the "rotate-sway-rotate" pathway, the $-CH_2Cl$ terminal group and a $-N^+(Me)_3$ tripod of TMCM molecules first rotate to form RS1 (Rotational State). Next, only the Cl-substituent terminal group clockwise sways a little to yield the paraelectric phase (denote as TS1 in Fig. 3a), and then further sways to form RS2. Lastly, the $-CH_2Cl$ group and $-N^+(Me)_3$ group cooperatively rotate to form ferroelectric phase FP2. The other phase-transition pathway is the "flip" one (the second row of Fig. 3a). Here, the "flip" refers to rotation of the whole TMCM molecule along the *c* axis to largely change its dipole orientation in TS2. Then, the $-CH_2Cl$ terminal group rotates counterclockwise and the $-N^+(Me)_3$ tripod also rotates counterclockwise at the same time to form the final ferroelectric phase FP3.

As shown in Fig. 3d and g, the TMCM-$MnCl_3$ crystal has nearly constant lattice parameters *b* and *c* in the "rotate-sway-rotate" mechanism, and constant lattice parameter *c* in the "flip" mechanism. The lattice parameter *a* elongates 0.4 Å from the ferroelectric phase FP1 to the TS1 phase along the "rotate-sway-rotate" pathway. Along the "flip" pathway, the lattice parameters *a* and *b* fluctuate within 0.8 Å. Similar to (pyrrolidinium)$MnCl_3$ and (3-pyrrolinium)$MnCl_3$, the 1D $MnCl_3$ chains here in the TMCM-$MnCl_3$ crystal are still too rigid to distort during the phase transition. But they can translate within the *ab*-plane as indicated by the relatively large change of lattice parameters *a* or *b* as shown in two phase-transition pathways (Fig. 3d and g). However, the motion of inorganic $MnCl_3$ chains is more complicated, compared to 1D ferroelectric $AMnCl_3$ perovskites with the quasi-planar organic cations, pyrrolidinium or 3-pyrrolinium. The lattice parameter β of $AMnCl_3$ crystals with the quasi-planar organic cations is unchanged, with a value of 90° during the phase transition, indicating that all the phases always keep orthorhombic. As shown in Fig. 3c and f, the lattice parameter β changes within the range of 86–94° along the two phase-transition pathways of TMCM-$MnCl_3$, resulting from combination of the translation of 1D $MnCl_3$ chains along the *a* direction and tilt of $MnCl_3$ chains along the *c* direction during the phase transition, coupled with motion of organic TMCM cations. This phase-transition behavior of 1D ferroelectric perovskites is quite different from the 3D perovskites, where organic cations are so small that the phase transition stems from distortion/transformation of inorganic corner-shared BX_6 octahedra.[20,21]

For these two phase-transition pathways, their energy diagrams are shown in Fig. 3b and e. Here, either phase-transition pathway

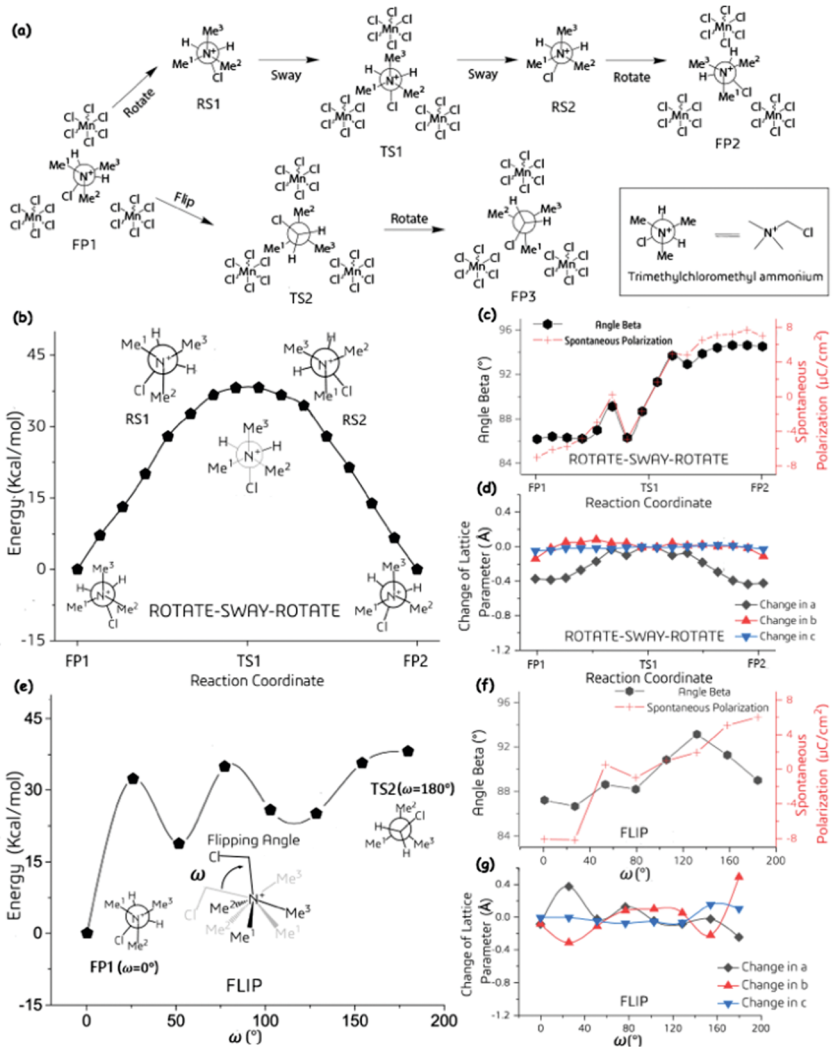

Fig. 3 (a) Molecular diagrams of mechanisms including the two "rotate-sway-rotate" and "flip" pathways; (b) variation of the energy with the reaction coordinate for the "rotate-sway-rotate" pathway; (c) variation of the lattice parameter β and spontaneous polarization (right axis) with the reaction coordinate for the "rotate-sway-rotate" pathway; (d) lattice parameter (*a*, *b*, and *c*) change for the "rotate-sway-rotate" pathway; (e) variation of the energy with flipping angle, ω, for the "flip" pathway; (f) variation of the lattice parameter β and spontaneous polarization (right axis) with ω for the "flip" pathway; (g) lattice parameter (*a*, *b*, and *c*) change for the "flip" pathway. The TMCM cation is expressed as its Newmann projection formula. FP, TS, and RS refer to the ferroelectric phase, transition state, and rotational state, respectively. The flipping angle (ω) is defined as the azimuthal angle of the N–C methylene bond relative to the N–C methylene bond of the TMCM cation in the initial FP1, as highlighted in the insets.

for the TMCM-$MnCl_3$ crystal would encounter a much higher energy barrier (about 40.0 kcal mol^{-1} for the "rotate-sway-rotate" pathway and 38.2 kcal mol^{-1} for the "flip" pathway) than that for the (pyrrolidinium)$MnCl_3$ or (3-pyrrolinium)$MnCl_3$ crystals. Although these energy barriers are not directly proportional to T_c, the higher energy barrier of the TMCM-$MnCl_3$ crystal can be qualitatively used to understand the high phase-transition temperature (406 K).[3] Notably, from FP1 or FP2 to TS1, the energy would gradually increase to 40.0 kcal mol^{-1} in Fig. 3b. Two ferroelectric phases, FP1 and FP2, are symmetric with each other. In the paraelectric phase, three "heavy" $-CH_3$s of the $-N^+(Me)_3$ tripod face towards three $MnCl_3$ octahedra. It is surely crowded to induce high-energy TS1. In both ferroelectric phases FP1 and FP2, three "heavy" $-CH_3$s occupy three "interstices" between triangular $MnCl_3$ chains. The rate-limiting transition of the "flip" mechanism from FP1 to TS2 is shown in Fig. 3e. This rate-limiting transition passes through two relatively low-energy intermediate states, and the energy has increasing tendency to reach 38.2 kcal mol^{-1} as the flipping angle (ω), defined as the azimuthal angle of the N–C methylene bond relative to the N–C methylene bond of a TMCM cation in the initial FP1, increases from 0° to 180°. The energy barriers for these two pathways are comparable to each other. Thus, the molecular motions corresponding to both proposed pathways would arise above the phase-transition temperature, consistent with the experimental XRD observation.[3]

According to two phase-transition pathways of TMCM-$MnCl_3$ crystals, the variations of spontaneous polarizations are shown in Fig. 3c and f. For either pathway, the calculated spontaneous polarization of the TMCM-$MnCl_3$ crystal is in the range of approximately -8.0 to 8.0 μC cm^{-2}, consistent with the

experimental value of 4.0 μC cm^{-2}.[3] The paraelectric phase along the "rotate-sway-rotate" pathway has zero polarization (Fig. 3c), and the state with nearly 90° flipping angle also has zero polarization (Fig. 3f). Switching from FP1, to TS1, to FP2 or from FP1 to TS2, the spontaneous polarization gradually increases in both cases (Fig. 3c and f). In addition to the "rotate-sway-rotate" pathway, P_s keeps almost unchanged during both "rotate" processes, but it changes considerably during the "sway" process. As discussed above, the dipole alignment of organic TMCM cations does contribute to P_s, and this dipole alignment is dependent on the inherent dipole moment and molecular motions. The dipole moment of TMCM is about 4.6 D, based on quantum chemistry calculations, about 1 D larger than those of two quasi-planar cations, pyrrolidinium and 3-pyrrolinium. In fact, three model systems exhibit comparable values of spontaneous polarization,[3,10,15] possibly because the large deformation of the unit cell induced by the translation or tilt of $MnCl_3$ chains gives an important contribution to the polarization.

Realization of piezoelectric response

Replacing the quasi-planar pyrrolidinium or 3-pyrrolinium molecules by the quasi-spherical TMCM molecule, 1D ferroelectric HOIPs can be endowed with strong piezoelectricity.[3,10,15] The piezoelectricity can be evaluated by the coefficient d_{33} that describes the capability of a material to generate charges on the plane normal to the applied strain.[3] If a material exhibits a strong piezoelectric response, the variation of microscopic lattice parameters with either external stimulus, *e.g.*, temperature or strain, would be a sensitive signal. Here, the temperature is used to assess the piezoelectric response of 1D ferroelectric HOIPs in light of the temperature-induced phase transition. For (pyrrolidinium)$MnCl_3$ and (3-pyrrolinium)$MnCl_3$ crystals, the variations of the lattice parameters, *a*, *b*, or *c*, along the phase-transition pathways from the ferroelectric phase to paraelectric phase exhibit a similar tendency (Fig. 2d and e). Compared to the "rotate-sway-rotate" pathway of TMCM-$MnCl_3$ crystals, its lattice parameters, *a*, *b*, and *c*, change less than those of (pyrrolidinium)$MnCl_3$ and (3-pyrrolinium)$MnCl_3$ crystals. Only *a* varies within 0.4 Å (Fig. 3d). Remarkably, the piezoelectric TMCM-$MnCl_3$ crystal exhibits a quite large change of lattice parameter β as shown in Fig. 3c and f. For the "rotate-sway-rotate" phase transition pathway, β keeps unchanged during the "rotate", and rapidly increases from 86° to 94° during the "sway" (Fig. 3c). Note that β = 90° for the paraelectric phase. For the "flip" pathway, the change of β is less regular, but still varies within the range of 86°–94° (Fig. 3f). Notably, the (pyrrolidinium)$MnCl_3$ and (3-pyrrolinium)$MnCl_3$ crystal, exhibiting the weak piezoelectric response, remain orthorhombic in both experiments[10,15] and our theoretical geometry optimization. Hence, the variation of lattice parameter β during the phase transition can be used as a semi-quantitative measure of the piezoelectricity of 1D perovskites.

In a previous work, You *et al.* showed that the strongest piezoelectric response is along the [102] direction of the TMCM-$MnCl_3$ crystal,[3] the same as the direction of the largest polarization. We propose that if the stress is applied along the [102] direction of the TMCM-$MnCl_3$ crystal for a ferroelectric phase with $\beta > 90°$ (Fig. 4), this crystal could turn into a paraelectric phase with β = 90°. This process can be referred to as the "rotate-sway-rotate" pathway (Fig. 3a–d). During this phase transition, the energy increases, β decreases, and *a* becomes larger. Thus, TMCM cations would reorient their terminal group due to X···X interaction, and slide a little along the *a* direction in response to the applied stress as indicated in Fig. 4. Under the stress, the paraelectric phase would be further switched to a low-energy ferroelectric phase with $\beta < 90°$. The initial and final ferroelectric phases are symmetric with one another. The whole process can be described analogically by a roly-poly toy in Fig. 4. Here, our proposed roly-poly model also highlights the role of lattice parameter β in describing the piezoelectricity of 1D ferroelectric HOIPs. Note that the lattice parameters, especially for β as the main factor, have been used previously to describe the elastic behavior of a single crystal under compression.[22] For our molecular design of new 1D ferroelectric/piezoelectric HOIPs, the variation of lattice parameter β during the phase transition can be employed as well to evaluate the piezoelectricity of these materials.

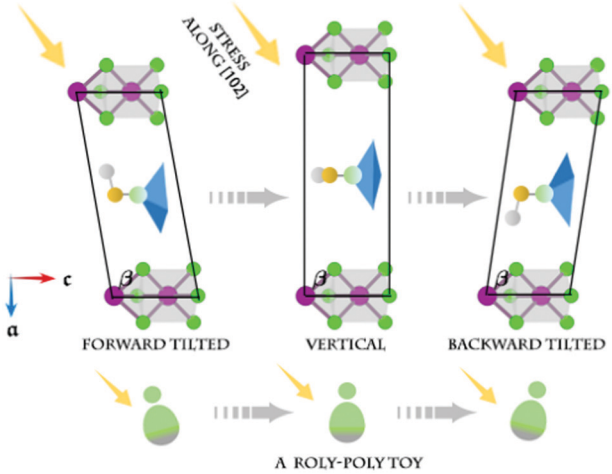

Fig. 4 The roly-poly model (lower panels) developed to understand the stress-induced piezoelectric response of TMCM-$MnCl_3$ crystals (see upper panels). The stress (yellow arrows) is applied along the [102] direction of the crystal. 1D chains with purple and green atoms represent $MnCl_3$ anions. The tripod model with a terminal group denotes the TMCM cation. Here, the relative translation and tilt of inorganic chains are clearly seen during the phase transition.

Molecular design of potential 1D ferroelectric HOIPs

Proposed design strategy. As discussed above, to endow 1D ferroelectric HOIPs with excellent piezoelectricity, delicate chemical modification on polar organic cations should be made to attain large change of lattice parameter β during its phase transition. First, we derive 15 1D HOIPs and further theoretically investigate their ferroelectricity/piezoelectricity-related phase transitions, as summarized in Table S2 (ESI†). We should emphasize that all designs are based on slight modification of the organic cation, TMCM, in the 1D ferroelectric $AMnCl_3$ perovskite. The TMCM molecules possess a

mirror symmetry together with a tripod geometry, which fit well with neighboring $MnCl_3$ chains. Correspondingly, the phase transition of the $AMnCl_3$ crystal would obey the symmetry principle from polar space group $Cmc2_1/Cc$ (ferroelectric phase) to nonpolar space group $P6_3/mmc$ (paraelectric phase). Using our successful/unsuccessful theoretical designs (see Table S2, ESI†), we can draw some design strategies for future experimental confirmation: (1) an effective approach for the molecular design is to make chemical modification of the TMCM molecule as slight as possible. The volume (or the size) of the cations is strongly limited by the 3D-linked MX_3 octahedra in traditional 3D HOIPs.[23] Unlike 3D perovskites, the limitation in the size of organic cations in 1D perovskites is rather small due to the extension along the direction of the 1D $MnCl_3$ chains, as shown by the identified forty-six 1D HOIPs (Table S3, ESI†). Indeed, the organic cations for 1D perovskites can be as large as (*S*)-β-phenethyl-ammonium,[24] *N*-butylquinolinium,[25] and benzyl-(triethyl)ammonium.[26] However, if organic cations change too much in size, it would largely alter the crystal packing to result in space groups that do not meet the symmetry principle for possible ferroelectric-to-paraelectric phase transition, as shown by Table S3 (ESI†) in that only a few perovskites have the polar space groups for possible ferroelectric states, while organic cations in these perovskites generally have a combined tripod group and terminal group similar to TMCM molecules. So we just tested slight modification of the model organic cation, TMCM. Successful design is achieved by substituting halogen atoms, F or Br, for Cl (see Table S2, ESI†). Similar Br-substituted piezoelectric TMBM-$MnBr_3$ has been synthesized in an experiment,[12] which supports our proposed design principle. The F or Br-substituted $AMnCl_3$ crystals do not exhibit excellent piezoelectricity like TMCM-$MnCl_3$, but still possess good ferroelectricity (larger spontaneous polarization; Table S2, ESI†) for TMFM-$MnCl_3$ and high phase-transition temperature (with slightly higher phase transition barrier as shown in Table S2, ESI†) for TMBM-$MnCl_3$, compared to the TMCM-$MnCl_3$ crystal.

(2) In order to obtain strong piezoelectricity for 1D ferroelectric perovskites, the design principle is to balance the sizes of the tripod group and terminal group of TMCM-analogical organic cations. As shown in Fig. 3b and c, rapid change in β is seen in the ''sway'' process. Thus, a possible and efficient way to enlarge β is through modifying three $-CH_3$s of the tripod groups or the $-CH_2Cl$ terminal group, in view of the highly confined triangular space made by three face-sharing $MnCl_3$ chains. Even though the ''sway'' process can be largely influenced by the size of the terminal group, and in turn, the change of terminal group significantly influences the β change, simply increasing the size of the terminal group would not work well. As shown by the example, trimethyl-trimethylsilanyloxymethyl-ammonium, in Table S2 (ESI†), keeping the $-N(CH_3)_3$ tripod group unchanged while replacing the $-CH_2Cl$ terminal group by $-CH_2OSiMe_3$ can cause a design failure. Hence, the key point is to balance the sizes of the terminal group and tripod group. How to balance the sizes of the two side groups in the molecular design of organic cations, however, is a challenge. Even with changing the tripod group and terminal group, some designs may fail due to space matching issues, as exemplified by 4-(2,2,2-trifluoro-ethyl)-hexahydro-pyrrolizinium in Table S2 (ESI†). However, when the terminal group is still $-CH_2CF_3$ while the tripod group becomes smaller, the design of organic cation, 1-methyl-1-(2,2,2-trifluoro-ethyl)-pyrrolidinium, is successful. This $AMnCl_3$ crystal behaves ferroelectric and piezoelectric but with a low phase transition temperature. We also attempted to change two methyl groups of a tripod group into ethyl groups, and then modify the terminal group to be $-CH_2CH_2F$ to achieve the size match of the tripod group and terminal group, and finally obtained the $AMnCl_3$ crystal with room-temperature ferroelectricity and excellent piezoelectricity, superior to TMCM-$MnCl_3$ (see below for detailed discussion).

(3) It is necessary to balance subtle interactions within 1D HOIPs. For trimethyl-(2,2,2-trichloro-ethyl)-ammonium (Me_3N^+–CH_2CCl_3) and bromomethyl-tris-trichloromethyl-ammonium ($(CCl_3)_3N^+$–CH_2Br), both cations suffer breaking of C–Cl bonds even during geometry optimization of the $AMnCl_3$ crystals, which may be due to either strong Cl–Cl halogen bonding, Mn–Cl interaction, or electronegativity of –a CCl_3 group. We observed that Cl atoms first move near other Cl atoms of the $MnCl_3$ chain and then move towards the Mn ions. Furthermore, for bromomethyl-bis-chloromethyl-methyl-ammonium ($Me(ClCH_2)_2N^+$–CH_2Br), less Cl atoms in the organic cation can make geometry optimization of ferroelectric/paraelectric phases successful, but still fail the CI-NEB calculations. Overall, it seems that a successful design of organic cations is quite sensitive to subtle interactions within 1D ferroelectric HOIPs. Still using $-N(CH_3)_3$ as the tripod group, substituting $-CH_2CBr_3$ for $-CH_2CCl_3$ as the terminal group to tune the weak interaction between organic cations and inorganic chains can make geometry optimization and CI-NEB calculations successful, but this design still leads to a phase transition energy barrier as high as >300 kcal mol^{-1}, since this design does not meet the second principle, *i.e.*, size matching of a terminal group and tripod group. If we continue decreasing the size of the terminal group from $-CH_2CBr_3$ to $-CH_2CF_3$, the $AMnCl_3$ crystal can finally entail the high-temperature ferroelectricity, outperforming the ferroelectricity of three other model systems (see below for detailed discussion). Here, more electronegative F atoms, with poorer polarization ability, would contribute to strong ferroelectricity and high phase transition energy barrier.

(4) Organic cations should not include active hydrogen. We then designed organic cation, trimethyl-sulfomethyl-ammonium (Me_3N^+–CH_2SO_3H), and obtained ferroelectric and paraelectric phases of the $AMnCl_3$ crystal with reference to the ferroelectric and paraelectric phases of TMCM-$MnCl_3$ crystals. We estimated a β change of about 5.3° and an energy difference, between the two states, of approximately 40 kcal mol^{-1}. The failure of CI-NEB calculation to connect the ferroelectric and paraelectric phases is ascribed to the leaving of the active hydrogen of $-SO_3$–H to interact with the nearby Cl atoms of $MnCl_3$ anions for intermediate states inserted in the CI-NEB calculations. This result implies that the active hydrogen in organic cations is unlikely to realize the synthesis of 1D ferroelectric $AMnCl_3$ crystals. A further design of Me_3N^+–CH_2SO_3Me to replace the active hydrogen atom by methyl

gives the corresponding $AMnCl_3$ crystal, which may be synthesized with weak ferroelectricity, good piezoelectricity, and very high phase transition temperature.

(5) The tendency of organic cations coordinated with Mn atoms in the anionic chains should be avoided. For trimethyl-(2-oxo-ethyl)-ammonium(Me_3N^+–CH_2CHO), the failure of geometry optimization of the $AMnCl_3$ crystal is likely due to the carbonyl group's weak interaction with Mn atoms. But the lack of carbonyl O atoms in Me_3N^+–CH_2NO_2 allows the $AMnCl_3$ crystal to gain super strong piezoelectricity and super high phase transition temperature, but without ferroelectricity.

Spotlighting two potential candidates. Based on the strategy elucidated above, seven new 1D ferroelectric HOIPs are designed as potential candidates (see Table S2, ESI†). Among them, two new TMTFE-$MnCl_3$ and DEMFE-$MnCl_3$ crystals (Fig. 1), are highlighted, because both give rise to the strongest room-temperature ferroelectricity or latent piezoelectricity (see Fig. 5). The phase-transition mechanism for both crystals can refer to the "rotate-sway-rotate" pathway of TMCM-$MnCl_3$ crystals (Fig. 3a). Thus, the energy changes of TMTFE-$MnCl_3$ and DEMFE-$MnCl_3$ crystals during the phase transitions are shown in Fig. 5a and d, respectively. One may see that the total size of DEMFE is larger than TMTFE, but the terminal group (–CH_2CH_2F) of DEMFE is smaller than that (–CH_2CF_3) of TMTFE. As shown in Fig. 5, the DEMFE-$MnCl_3$ crystal results in a smaller barrier and a larger β change compared to the TMTFE-$MnCl_3$ crystal. The energy barrier is about 46.4 kcal mol^{-1} for the TMTFE-$MnCl_3$ crystal (Fig. 5a), and about 20.4 kcal mol^{-1} for the DEMFE-$MnCl_3$ crystal (Fig. 5d).

Although the energy barrier of phase transition is not directly proportional to T_c, the higher energy barrier still implies higher T_c.[11,18] This point is also confirmed by the higher T_c of the TMCM-$MnCl_3$ crystal with a high energy barrier of about 40.0 kcal mol^{-1}, compared to those of (pyrrolidinium)-$MnCl_3$ and (3-pyrrolinium)$MnCl_3$ crystals. The energy barrier of TMTFE-$MnCl_3$ crystals is as high as about 46.4 kcal mol^{-1}, even higher than that of TMCM-$MnCl_3$ crystals. Thus, the newly designed TMTFE-$MnCl_3$ crystal is expected to exhibit higher T_c than T_c = 406 K of the TMCM-$MnCl_3$ crystal.[3] Meanwhile, the energy barrier of the DEMFE-$MnCl_3$ crystal is 20.4 kcal mol^{-1}, which is quite a bit lower than that of TMCM-$MnCl_3$ crystals. However, the DEMFE-$MnCl_3$ crystal exhibits much larger polarization during phase transition, which would also contribute to its phase transition temperature T_c according to the Landau–Devonshire phase transition theory.[19] The predicted high T_c for the newly designed TMTFE-$MnCl_3$ and DEMFE-$MnCl_3$ crystals can be further supported by the polarizability–temperature curves shown in Fig. S4 (ESI†). The temperature-dependent polarizability curves are computed according to the first-principles calculations of phase-transition energies (Fig. 2b, 3b, 5a, and d) and polarizations

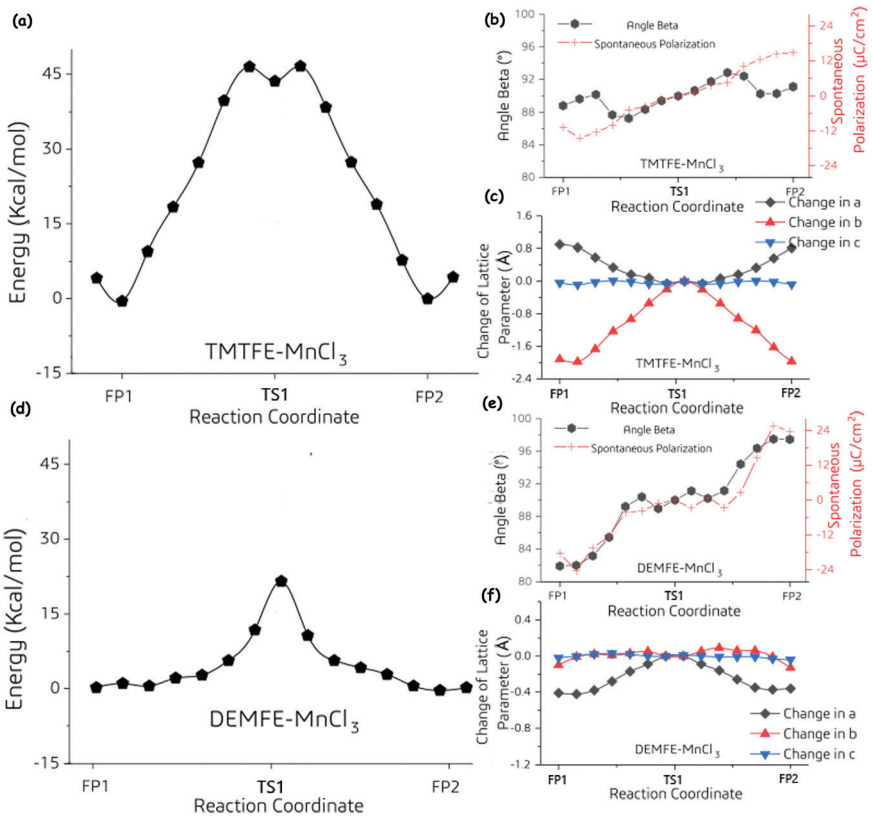

Fig. 5 Phase transition characteristics of TMTFE-$MnCl_3$ and DEMFE-$MnCl_3$ crystals: variation of energy with reaction coordinate for (a) TMTFE-$MnCl_3$ and (d) DEMFE-$MnCl_3$ crystals; variation of lattice parameter β and spontaneous polarization with reaction coordinate for (b) TMTFE-$MnCl_3$ and (e) DEMFE-$MnCl_3$ crystals; and lattice parameter (*a*, *b*, and *c*) change for (c) TMTFE-$MnCl_3$ and (f) DEMFE-$MnCl_3$ crystals. FP and TS indicate ferroelectric phase and transition state, respectively.

(Fig. 2c, 3c, 5b, and e) and the Boltzmann statistics formula. Based on the temperature-dependent polarizability curves (Fig. S4, ESI†), TMTFE-$MnCl_3$ and DEMFE-$MnCl_3$ crystals are expected to achieve notably higher T_c than three model systems (whose T_cs are in the range of 291–406 K),[3,10,15] as the values at the inflection points, seving as an estimation of the transition temperatures of TMTFE-$MnCl_3$ and DEMFE-$MnCl_3$ crystals, are surely higher than those of the three model systems.

As shown in Fig. 5b and e, the calculated spontaneous polarization of TMTFE-$MnCl_3$ crystals is in the range of -14.6 to 15.8 μC cm^{-2}, and that of DEMFE-$MnCl_3$ crystals is in the range of -25.6 to 24.3 μC cm^{-2} during the phase transition. The estimated spontaneous polarizations of both newly designed crystals appear to be higher than those of 1D ferroelectric HOIPs, measured from the experiments.[3,9–16] Although the lattice parameter β of TMTFE-$MnCl_3$ crystals ($\pm 1.2^\circ$) changes a little (Fig. 5b), other lattice parameters of the crystal, especially a (± 0.9 Å) and b (± 2.0 Å) (Fig. 5c), do change a lot. The TMTFE-$MnCl_3$ crystal is probably piezoelectric along the [100] or [010] directions. The DEMFE-$MnCl_3$ crystal exhibits a larger β range ($\pm 7.8^\circ$) (Fig. 5e), compared to the model system of TMCM-$MnCl_3$. The change of its lattice parameters a, b, and c (Fig. 5f) is similar to that of TMCM-$MnCl_3$ crystals (Fig. 3d). The lattice parameter a changes within 0.4 Å, while b and c are unchanged. To the best of our knowledge, the two candidates, TMTFE-$MnCl_3$ and DEMFE-$MnCl_3$ crystals, could be 1D ferroelectric HOIPs with the largest polarization and the highest T_c, especially with the strongest piezoelectricity for DEMFE-$MnCl_3$ crystals, compared to the reported systems.[3,10,15]

Conclusions

On the basis of first-principles calculations, the ferroelectricity/piezoelectricity-related phase transition mechanisms are explored in detail for three model systems of 1D ferroelectric HOIPs, (pyrrolidinium)$MnCl_3$, (3-pyrrolinium)$MnCl_3$, and TMCM-$MnCl_3$. The mechanistic study allows us to confirm the computed spontaneous polarizations of the three model systems to be consistent with the experimental values, and to evaluate the phase transition temperatures based on the temperature-dependent polarizability analyses and the piezoelectricity by using the variable lattice parameters, especially β, during the phase transition. By virtue of a comprehensive survey of experimental 1D HOIPs and a dedicated trial of theoretical design, seven ferroelectric/piezoelectric potential candidates are identified, especially for the two of them, trimethyl(2,2,2-trifluoroethyl)ammonium trichloromanganese(II) (TMTFE-$MnCl_3$) and diethylmethyl(2-fluoroethyl)ammonium trichloromanganese(II) (DEMFE-$MnCl_3$). Our theoretical simulations predict that both newly designed perovskites would have ultra-large spontaneous polarization, excellent ferroelectricity with transition temperature likely higher than 406 K, and strong piezoelectricity, especially for the DEMFE-$MnCl_3$ crystal. Thus, our prediction, that the TMTFE-$MnCl_3$ and DEMFE-$MnCl_3$ crystals may outperform all previously reported 1D ferroelectric HOIPs, must await future experiments for confirmation. If confirmed, our proposed design strategy can be applied for the design of many other 1D HOIPs.

Conflicts of interest

There are no conflicts to declare.

Acknowledgements

We thank Professor Liang Ma and Ms Yinglu Jia for valuable discussions. This work was supported by the National Natural Science Foundation of China (Grant No. 21603097), the Natural Science Foundation of Jiangsu Province (Grant No. BK20160613), and the Fundamental Research Funds for the Central Universities. The computation was performed in the High Performance Computing Center (HPCC) in Nanjing University. XCZ is supported by UNL Holland Computing Center.

Notes and references

1 Y. Zhang, W. Jie, P. Chen, W. Liu and J. Hao, *Adv. Mater.*, 2018, **30**, 1707007.
2 S. Horiuchi, F. Ishii, R. Kumai, Y. Okimoto, H. Tachibana, N. Nagaosa and Y. Tokura, *Nat. Mater.*, 2005, **4**, 163.
3 Y.-M. You, W.-Q. Liao, D. Zhao, H.-Y. Ye, Y. Zhang, Q. Zhou, X. Niu, J. Wang, P.-F. Li, D.-W. Fu, Z. Wang, S. Gao, K. Yang, J.-M. Liu, J. Li, Y. Yan and R.-G. Xiong, *Science*, 2017, **357**, 306.
4 J. Berry, T. Buonassisi, D. A. Egger, G. Hodes, L. Kronik, Y.-L. Loo, I. Lubomirsky, S. R. Marder, Y. Mastai, J. S. Miller, D. B. Mitzi, Y. Paz, A. M. Rappe, I. Riess, B. Rybtchinski, O. Stafsudd, V. Stevanovic, M. F. Toney, D. Zitoun, A. Kahn, D. Ginley and D. Cahen, *Adv. Mater.*, 2015, **27**, 5102.
5 W. S. Yang, B.-W. Park, E. H. Jung, N. J. Jeon, Y. C. Kim, D. U. Lee, S. S. Shin, J. Seo, E. K. Kim, J. H. Noh and S. I. Seok, *Science*, 2017, **356**, 1376.
6 N. J. Jeon, H. Na, E. H. Jung, T.-Y. Yang, Y. G. Lee, G. Kim, H.-W. Shin, S. Il Seok, J. Lee and J. Seo, *Nat. Energy*, 2018, **3**, 682.
7 B. Saparov and D. B. Mitzi, *Chem. Rev.*, 2016, **116**, 4558.
8 W. Li, Z. Wang, F. Deschler, S. Gao, R. H. Friend and A. K. Cheetham, *Nat. Rev. Mater.*, 2017, **2**, 16099.
9 H.-Y. Ye, Y. Zhang, D.-W. Fu and R.-G. Xiong, *Angew. Chem., Int. Ed.*, 2014, **53**, 11242.
10 Y. Zhang, W. Q. Liao, D. W. Fu, H. Y. Ye, Z. N. Chen and R. G. Xiong, *J. Am. Chem. Soc.*, 2015, **137**, 4928.
11 P.-F. Li, W.-Q. Liao, Y.-Y. Tang, H.-Y. Ye, Y. Zhang and R.-G. Xiong, *J. Am. Chem. Soc.*, 2017, **139**, 8752.
12 W.-Q. Liao, Y.-Y. Tang, P.-F. Li, Y.-M. You and R.-G. Xiong, *J. Am. Chem. Soc.*, 2017, **139**, 18071.
13 W.-Q. Liao, Y.-Y. Tang, P.-F. Li, Y.-M. You and R.-G. Xiong, *J. Am. Chem. Soc.*, 2018, **140**, 3975.
14 Y. Zhang, W. Q. Liao, D. W. Fu, H. Y. Ye, C. M. Liu, Z. N. Chen and R. G. Xiong, *Adv. Mater.*, 2015, **27**, 3942.

15 H. Y. Ye, Q. Zhou, X. Niu, W. Q. Liao, D. W. Fu, Y. Zhang, Y. M. You, J. Wang, Z. N. Chen and R. G. Xiong, *J. Am. Chem. Soc.*, 2015, **137**, 13148.
16 W.-J. Xu, C.-T. He, C.-M. Ji, S.-L. Chen, R.-K. Huang, R.-B. Lin, W. Xue, J.-H. Luo, W.-X. Zhang and X.-M. Chen, *Adv. Mater.*, 2016, **28**, 5886.
17 Z. Wang, Y. Lu, H. P. Chen and J. Z. Ge, *Inorg. Chem.*, 2017, **56**, 7058.
18 Q. Pan, Z.-B. Liu, Y.-Y. Tang, P.-F. Li, R.-W. Ma, R.-Y. Wei, Y. Zhang, Y.-M. You, H.-Y. Ye and R.-G. Xiong, *J. Am. Chem. Soc.*, 2017, **139**, 3954.
19 P. Chandra and P. B. Littlewood, *A Landau Primer for Ferroelectrics in Physics of Ferroelectrics: A Modern Perspective*, ed. K. M. Rabe, Ch. H. Ahn and J.-M. Triscone, Springer-Verlag, Berlin, 2007, pp. 69–116.
20 K. P. Ong, T. W. Goh, Q. Xu and A. Huan, *J. Phys. Chem. Lett.*, 2015, **6**, 681.
21 L. Z. Tan, F. Zheng and A. M. Rappe, *ACS Energy Lett.*, 2017, **2**, 937.
22 K. J. Gagnon, C. M. Beavers and A. Clearfield, *J. Am. Chem. Soc.*, 2013, **135**, 1252.
23 G. Kieslich, S. Sun and A. K. Cheetham, *Chem. Sci.*, 2014, **5**, 4712.
24 D. G. Billing and A. Lemmerer, *Acta Crystallogr., Sect. E: Struct. Rep. Online*, 2003, **59**, m381.
25 H.-H. Li, Z.-R. Chen, L.-Q. Guo, K.-N. Ding, J.-Q. Li, C.-C. Huang and Z.-L. Cai, *Aust. J. Chem.*, 2007, **60**, 595.
26 Y. Niu, X. Chen, Y. Zhu and S. Li, *Sens. Actuators, B*, 2017, **242**, 632.